STEM CELLS®

Comparative Analysis of the Frequency and Distribution of Stem and Progenitor Cells in the Adult Mouse Brain

Mohammad G. Golmohammadi, Daniel G. Blackmore, Beatrice Large, Hassan Azari, Ebrahim Esfandiary, George Paxinos, Keith B. J. Franklin, Brent A. Reynolds and Rodney L. Rietze

This information is current as of April 29, 2008

The online version of this article, along with updated information and services, is located on the World Wide Web at:
http://www.StemCells.com/cgi/content/full/26/4/979

α AlphaMed Press

Comparative Analysis of the Frequency and Distribution of Stem and Progenitor Cells in the Adult Mouse Brain

MOHAMMAD G. GOLMOHAMMADI,[a,b,c] DANIEL G. BLACKMORE,[a] BEATRICE LARGE,[a] HASSAN AZARI,[a,b]
EBRAHIM ESFANDIARY,[b] GEORGE PAXINOS,[d] KEITH B. J. FRANKLIN,[e] BRENT A. REYNOLDS,[a]
RODNEY L. RIETZE[a]

[a]Queensland Brain Institute, The University of Queensland, Brisbane, QLD 4072, Australia,[b]School of Medicine,
Isfahan University of Medical Sciences, Isfahan 81744-176, Iran,[c]School of Medicine, Ardabil University of
Medical Sciences, Ardabil, Iran,[d]Prince of Wales Medical Research Institute, Randwick, NSW 2031,
Australia,[e]Department of Psychology, McGill University, Montreal, Quebec, Canada H3A 1B1

ABSTRACT

The neurosphere assay can detect and expand neural stem cells (NSCs) and progenitor cells, but it cannot discriminate between these two populations. Given two assays have purported to overcome this shortfall, we performed a comparative analysis of the distribution and frequency of NSCs and progenitor cells detected in 400 μm coronal segments along the ventricular neuraxis of the adult mouse brain using the neurosphere assay, the neural colony forming cell assay (N-CFCA), and label-retaining cell (LRC) approach. We observed a large variation in the number of progenitor/stem cells detected in serial sections along the neuraxis, with the number of neurosphere-forming cells detected in individual 400 μm sections varying from a minimum of eight to a maximum of 891 depending upon the rostral-caudal coordinate assayed. Moreover, the greatest variability occurred in the rostral portion of the lateral ventricles, thereby explaining the large variation in neurosphere frequency previously reported. Whereas the overall number of neurospheres (3730 ± 276) or colonies (4275 ± 124) we detected along the neuraxis did not differ significantly, LRC numbers were significantly reduced (1186 ± 188, 7 month chase) in comparison to both total colonies and neurospheres. Moreover, approximately two orders of magnitude fewer NSC-derived colonies (50 ± 10) were detected using the N-CFCA as compared to LRCs. Given only 5% of the LRCs are cycling (BrdU$^+$/Ki-67$^+$) or competent to divide (BrdU$^+$/Mcm-2$^+$), and proliferate upon transfer to culture, it is unclear whether this technique selectively detects endogenous NSCs. Overall, caution should be taken with the interpretation and employment of all these techniques. STEM CELLS 2008;26:979–987

Disclosure of potential conflicts of interest is found at the end of this article.

INTRODUCTION

It is now clear that the adult mammalian brain contains endogenous neural stem [1–3] and progenitor cells (together termed precursor cells) that replace lost populations of cells in at least two regions of the brain, the olfactory bulb and the hippocampus [4–8]. In light of continued neurogenesis and the unexpected ability of resident precursors to become activated following injury [9, 10], efforts are now focused on characterizing these cells so as to harness their regenerative capacity. Because of their rarity, an essential first step in understanding what factors regulate the actions of endogenous adult neural stem cells (NSCs) and their progeny is the elucidation of cell-specific markers.

Attempts to purify populations of endogenous adult NSCs from more differentiated, yet proliferative cell types (i.e., progenitor cells) based on their unique repertoire of cell surface antigens [11–14] or differential dye efflux [15, 16] using flow cytometry and the neurosphere assay (NSA) as a readout for stem cell activity have achieved only a moderate level of success. This is largely attributed to a combination of poor enrichment and, as discussed below, the overestimation of NSC numbers based on the erroneous belief that a one to one relationship exists between neurospheres and NSCs [17]. Furthermore, these purification strategies have typically been based on negative selection, thereby precluding the tracking of NSCs in vivo.

Two approaches have recently been described which may address these shortfalls and enable one to distinguish NSCs from more committed progenitor cells. The first is based on the concept that tissue stem cells can be identified by their relative mitotic quiescence [18–21]. By labeling the majority of a population of mitotically active cells with bromodeoxyuridine (BrdU) or another suitable marker of dividing cells, then chasing these cells for a period of time so as to dilute the label from fast cycling progenitor cells [22, 23], one can identify infrequently dividing or label-retaining cells (LRCs). This approach has been used to identify putative stem cells in the mammary gland, hair follicles, kidney [18, 20, 21, 24], and most recently, in the adult mouse brain [25, 26].

The second approach is an in vitro assay termed the neural colony forming cell assay (N-CFCA) [27], which is similar to

the NSA in that it employs a defined serum-free medium. However, it allows NSC-derived colonies to be discriminated from those not derived from NSCs based on the size of colony as only cells comprising the largest colonies (those >2.0 mm in diameter) exhibit the cardinal properties of bona fide NSCs in vitro. To date, the N-CFCA has been validated using both embryonic and adult-derived neural cells [28], and has been employed to demonstrate that the adult hippocampus does not contain a population of NSCs [29].

As a detailed investigation into the frequency and distribution of sphere-forming cells (SFCs) along the ventricular neuraxis has yet to be conducted, and in light of the novelty of the LRC approach and N-CFCA, we sought to perform a detailed analysis comparing these methodologies so as to determine their reliability in detecting populations of NSCs and their more restricted progeny (i.e., progenitor cells).

MATERIALS AND METHODS

Animals and Housing Conditions

Adult (6–8 weeks of age) male CBA mice (Animal Resource Centre, Nedlands, WA, http://www.arc.wa.gov.au) were housed with unlimited access to food and water, and treated in accordance with the Australian Code of Practice for the Care and Use of Animals for Scientific Purposes. The University of Queensland Animal Ethics Committee approved all experiments performed here.

Neural Cell Cultures

Naïve adult (6–8 weeks) CBA male mice were sacrificed by cervical dislocation, their brains harvested (olfactory bulbs intact) and cut coronally into 400 μm sections using a Leica VT 1,000s vibratome. Initial experiments demonstrated no significant difference in the distribution, frequency, or overall number of spheres/colonies generated in males versus females. As such, only male mice were used for all subsequent experiments.

Individual vibratome sections were collected serially starting at 4.28 mm rostral to Bregma and continuing to the level of the fourth ventricle [30]. Due to tissue degradation and abundant cell death it was not feasible to harvest and generate cultures from all 23 sections in a single brain. Rather, serial vibratome sections were harvested from either the rostral (sections 3–9), mid (sections 9–15), or caudal portions (sections 15–25) of each brain. Three brains were harvested for each of the rostral, mid, and caudal portions on three separate occasions ($n = 3$). Sections 9 and 15 represent overlapping sections (internal controls) and therefore $n = 6$. To ensure accuracy within and between experiments, every brain was sectioned at least to section 13, where the joining of the anterior commissure occurs (Bregma +0.14). Those brains where this landmark did not occur at section 13 were rejected.

The entire periventricular regions (PVR; a 3–5 cell thick region adjacent to the ependymal layer of the ventricles) was microdissected from each section under x2 magnification using an ultrafine scalpel. Harvested tissue was enzymatically brought to single cell suspension, filtered through a 40 μm nylon strainer, and initially cultured at a density of 3,500 viable cells/cm^2 in 6-well plates so as to determine the number of primary neurospheres generated in each 400 μm section as previously described [31]. In all cases, PVR tissue from individual sections was treated separately (i.e., never pooled). Whereas cell density varied between serial sections in subsequent experiments according to the prevalence of sphere forming cells, identical seeding densities were used in both the NSA and N-CFCA for individual matched coronal sections. In the case of the N-CFCA, single cell suspensions were enzymatically generated (as above), a cell count performed, and the appropriate cell numbers mixed with the serum-free N-CFCA medium containing supplements as described in the Neural Colony Forming Cell Assay kit (Stem Cell Technologies, Vancouver, BC, Canada, http://www.stemcell.com). Epidermal growth factor (EGF, 20 ng/ml, BD Bio-

sciences, Australia, http://www.bdbiosciences.com) and basic fibroblast growth factor (bFGF, 10 ng/ml, Roche, Basel, Switzerland, http://www.roche.com) were employed in all in vitro assays so as to include both EGF- and bFGF-responsive precursor cells.

Primary neurospheres were counted after 7–10 days in vitro (DIV) depending upon the growth rate of the particular cell population. Cultures were monitored until the average sphere size for the majority of the culture was about 180 μm (typically 8 DIV), at which time they were scored. As described in the product disclosure statement, cells cultured in the N-CFCA were fed at seven and 14 DIV, then counted at 21 DIV to allow for the maximal growth of the cells/colonies to enable a clear and obvious distinction of colony sizes. In both the neurosphere assay and the N-CFCA, only those clusters with a minimum diameter of 50 μm were scored.

To detect BrdU-immunoreactive (BrdU-IR) neurosphere-derived cells, three independent neurosphere cultures were generated from individual BrdU-recipient mice. Primary neurospheres were transferred 4 DIV from a T-25 flask to a single well of a 24-well plate pre-coated with cell-Tak (BD Biosciences). Following a 15 minute incubation at 37°C, neurospheres were fixed by the addition of 4% paraformaldehyde for 10 minutes, rinsed and processed for BrdU-IR cells as described above for tissue sections.

BrdU Injection Protocol and Tissue Processing

Adult (6–8 weeks of age) male CBA mice were administered intraperitoneal (i.p.) 150 μL (9 mg/ml, 45 mg/kg body weight) injections of BrdU (Sigma, St. Louis, http://www.sigmaaldrich.com) dissolved in 0.07 N NaOH in 0.9% NaCl every 2 hours for a period of 48 hours. Animals were sacrificed 30 minutes, or 1, 2, 3, 4, 6, 9, 12, 20 weeks after the last injection. Two separate cohorts of mice received BrdU injections and brains from three mice were processed at each time point.

After the appropriate survival period, mice were deeply anesthetized with sodium pentobarbitone (260 mg/kg), then transcardially perfused with 0.9% saline followed by 4.0% paraformaldehyde in 0.1 M phosphate buffer (pH 7.4). Brains were harvested, postfixed, and cryoprotected as previously described [7]. Serial frontal sections (14 μm) were cut (collecting every third section) with a Leica CM3050 cryostat, and mounted on SuperFrost Plus slides, dried at room temperature and stored at −20°C until needed. Sections were processed for dual-label BrdU immunocytochemistry essentially as previously described [7] labeling with the appropriate primary antibody; anti-S100β (1:500; Dako), anti-neuronal nuclei (NeuN, 1:100; Chemicon, Boronia, Australia, http://www.chemicon.com), anti-Ki67 (1:100; Novacastra, Newcastle, U.K., http://www.novocastra.co.uk), anti-BrdU (Accurate Chemical, Westbury, U.K., http://www.accuratechemical.com), anti-myelin basic protein (MBP, 1:250; Chemicon), anti-CD31, anti-CD45 (BD Bioscience, 1:150), and anti-mini-chromosomal marker-2 (Mcm-2, 1:200; Santa Cruz Biotech, Santa Cruz, CA, http://www.scbt.com), all diluted in 0.1 M PBS + 0.3% Triton + 10% normal goat serum. Sections were rinsed and then incubated with the appropriate secondary antibodies, goat anti-rabbit IgG (AlexaFluor 568, 1:500; Molecular Probes, Eugene, OR, http://probes.invitrogen.com), goat anti-mouse (AF 568, 1:500; Molecular Probes) or donkey anti-rat (AF 488, 1:300; Molecular Probes) for 1 hour at room temperature. Following completion of the first label, sections were processed for BrdU immunoreactivity. Coverslips were mounted using FluorSave (Calbiochem, San Diego, http://www.emdbiosciences.com).

For each individual brain harvested at each time point, the number of LRCs was determined for 23 individual 400 μm regions by subtracting the mean number of BrdU-IR differentiated cells (i.e., BrdU/NeuN, BrdU/S-100, BrdU/MBP) from the mean number of BrdU-IR cells detected in five individual tissue sections (14 μm/section), spanning a 420 μm segment of the brain.

Images were captured on a Canon EOS digital camera using an Olympus Axiophot upright fluorescence microscope. Brightness and contrast were adjusted using Adobe Photoshop CS3.

Statistical Analysis

Factorial design analysis of variance (ANOVA) or Student's two tailed, unpaired, t-tests were used to analyze data as appropriate (Prism 4, Graphpad Software, San Diego, http://www.graphpad.

com). Significant ANOVA values were followed by post hoc comparisons of individual means using the Tukey method where appropriate. All values are expressed as mean±standard error of the mean unless otherwise indicated. The level of significance for all comparisons was $p < .01$.

RESULTS

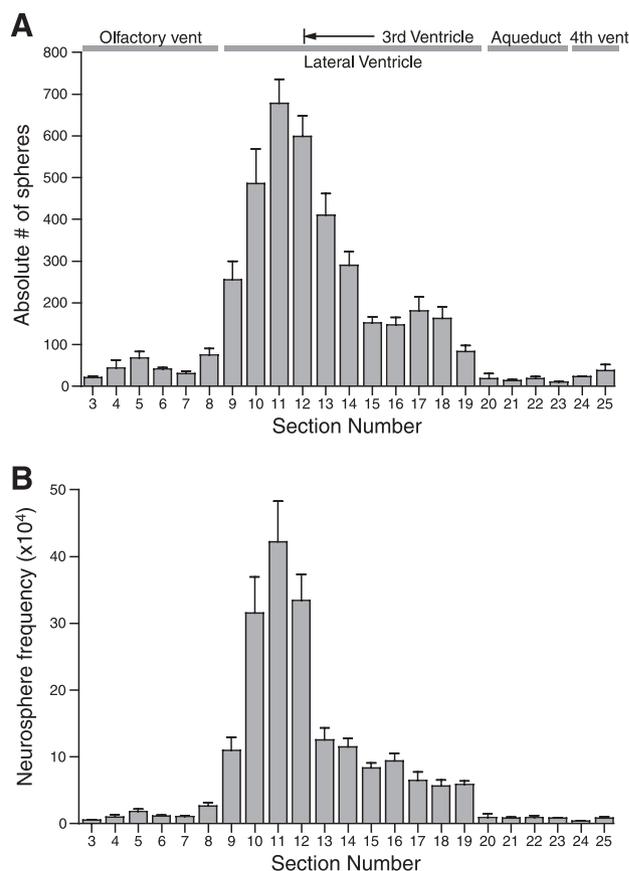### Frequency and Distribution of Neurosphere-Forming Cells

Earlier work has demonstrated that constitutively proliferating cells [32, 33] and SFCs reside along the entire PVR, a 3–5 cell layer thick region of tissue directly adjacent to the ependymal lining of the lateral, third, and fourth ventricles [34, 35] as well as the olfactory bulb [36]. Whereas cell genesis and neural precursor cells have been reported in a number of regions of the adult brain outside the PVR [37], the PVR represents the only region where adult NSCs have been unequivocally demonstrated to reside [35]. As such, we restricted our analysis of the frequency of NSCs and more restricted progenitor cells to the PVR of the adult brain.

To determine the frequency of SFCs, brains were harvested from naïve adult (6–8 week) mice and serially vibratome sectioned (400 μm/section) starting at the level of the olfactory bulb (4.28 mm rostral to Bregma [30]). The PVR was then micro-dissected from each section, enzymatically dissociated, and the resulting single cell suspension transferred to neurosphere culture conditions using the mitogens EGF and bFGF [1, 31]. Both mitogens were employed here and in all subsequent in vitro assays so as to include both EGF and bFGF-responsive precursor cells. After 7-10 DIV, the absolute number of SFCs in each region were counted and plotted according to their rostral-caudal distribution. As shown in Figure 1 and consistent with prior work [34, 36], SFCs were detected in the olfactory bulb and throughout the ventricular neuraxis. Also consistent with prior work, neither the absolute number (Fig. 1A) nor frequency (absolute number of SFCs/10^4 cells plated, Fig. 1B) of SFCs was uniform along the length of the neuraxis [34, 36]. Rather, the greatest number and frequency of SFCs were detected in rostral (sections 9–14), rather than caudal (sections 15–19) portions of the lateral ventricles. Indeed, only ~11% of the total number of SFCs detected (3,730 ± 276 in total, $n = 3$) were found outside this region.

Frequency and Distribution of Colony-Forming Cells

Concurrent with the determination of SFC frequency, we also cultured PVR cells harvested from anatomically matched vibratome sections in the N-CFCA [27], once again using the mitogens EGF and bFGF. After 21 DIV, the overall number of colonies generated from tissue harvested from each section was counted and the results plotted according to rostral-caudal position (Fig. 2A). Attesting to the detection of similar populations of neural precursor cells, no significant difference was observed between the overall number of SFCs (3,730 ± 276, Fig. 1A) and colony-forming cells (4,275 ± 124, $p = .08$, $n = 3$, Student's t-test). Indeed, the distribution and frequency of colony generation mirrored almost exactly that of neurosphere generation along the entire neuraxis, with a section-by-section comparison of the absolute number of sphere-forming versus colony-forming cells revealing that only sections 3, 6, 7, 21 and 23 differed significantly (Fig. 2A, $p < .01$, $n = 3$, Student's t-test).

Because of the ability of the N-CFCA to discriminate between neural stem and progenitor cells based on the proliferative capacity of NSCs [28, 29], we also measured the diameter of all

Figure 1. Distribution and frequency of neurosphere-forming cells along the ventricular neuraxis. Histogram(s) showing the absolute number (**A**) and frequency (**B**) of primary neurospheres that can be generated from PVR cells in individual serial vibratome sections (400 μm) starting at the level of the olfactory bulb (section 3, 4.28 mm rostral to Bregma). The majority of SFCs are located within the portion of the PVR traditionally dissected (i.e., section 9–14; start of the rostral migratory stream to the level of the optic chiasm). The large variation in the absolute number of SFCs within this region [253 ± 72 (section 9, $n = 6$) versus 676 ± 76 (section 11, $n = 3$)] coupled with the significant decline in the number of SFCs as one proceeds from the lateral ventricle (section 11) towards the rostral migratory stream (section 8, $p < .01$, Student's t-test) explains the variation in the number of neurospheres previously reported by individual groups employing the same basic technique (Mean ± SEM, $n = 3$ mice harvested for each section except sections 9 and 15, where $n = 6$).

of the colonies generated, and plotted the number of large colonies (i.e., >2 mm) detected in each section (Fig. 2B). As expected, because of the relative rarity of NSCs as compared to more differentiated proliferative progenitors, the total number of large (i.e., NSC-derived) colonies represented only a fraction (1.2% or 50 ± 10, $n = 3$) of the overall number of colonies detected. Somewhat unexpectedly, large colonies were not detected in four regions along the ventricular neuraxis (sections 10, 20, 23 and 25) corresponding to plates 20, 55, 65, and 69 of the mouse atlas [30] respectively.

Whereas the absence of large colonies in the more caudal sections may be explained in part by the low number of colony-forming (Fig. 2A) and SFCs (Fig. 1A) in the region(s), this cannot explain their absence in the rostral portion of the lateral ventricle. Indeed, an average of 563 ± 14 colonies (Fig. 2A, mean ± SEM, $n = 3$) and 483 ± 84 neurospheres (Fig. 1A, $n = 3$) were generated in this 400 μm section (section 10). Therefore, to investigate whether this observation could be attributed to a peculiarity in the N-CFCA, we generated neurosphere
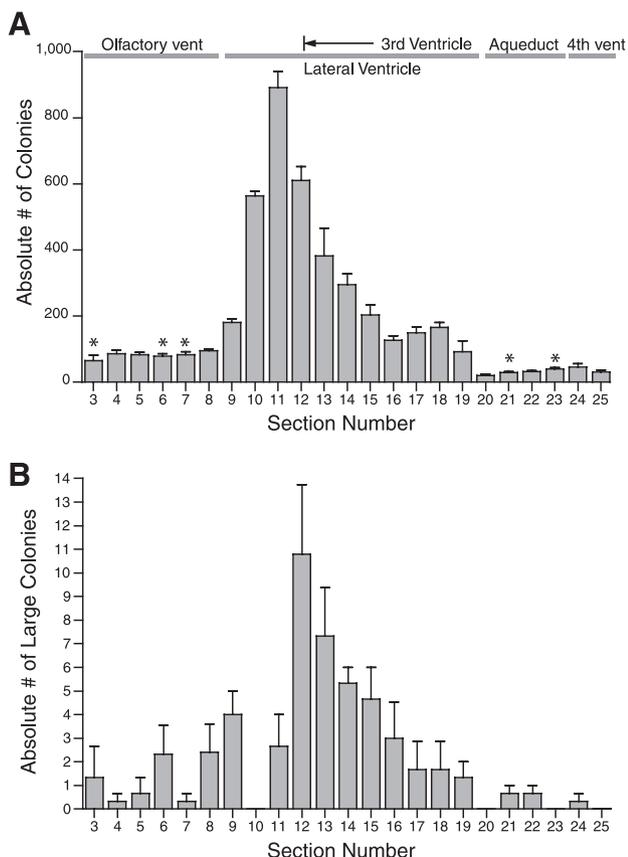
Figure 2. Distribution and frequency of colony-forming cells along the ventricular neuraxis. **(A)** Histogram showing the overall number of colonies (regardless of size) detected in individual serial vibratome sections (400 μm) starting at the level of the olfactory bulb (section 3, 4.28 mm rostral to Bregma). Similar to the findings for SFCs (Fig. 1A), colony number declines significantly as one proceeds rostrally from section 11 to section 8 ($p < .01$, $n = 3$, Student's t-test). Colony-forming cell frequency was significantly different from SFC frequency only in sections denoted by an asterisk ($p < .01$, $n = 3$, Student's t-test). The total number of colonies (4,275 $\pm$ 124, mean $\pm$ SEM, $n = 3$) was not significantly different from the overall number of SFCs detected ($p = .08$, Student's t-test). **(B)** Frequency of large (> 2 mm) colonies detected along the neuraxis. Approximately 54% of the 50 $\pm$ 10 (mean $\pm$ SEM, $n = 3$) NSC-derived colonies detected along the neuraxis are located in sections 9–14. Unlike SFCs (Fig. 1A), large colonies were not detected in sections 10, 20, 23, or 25 suggesting an absence of NSCs in these regions.

cultures from PVR tissue harvested from 400 μm vibratome sections 9–13 ($n = 3$ cultures per section) and assayed for the cardinal stem cell properties of extensive proliferation and self-renewal by attempting to expand these cultures for at least five passages. Consistent with an absence of bona fide NSCs in the region, none of the neurosphere cultures generated from section 10 could be passaged more than three times ($n = 3$), whereas all of those generated from adjacent sections could be serially passaged a minimum of five times.

Frequency and Distribution of LRCs Along the Ventricular Neuraxis

The retention of BrdU is considered adequate to quantify pro-liferative (yet relatively quiescent) NSCs as opposed to rapidly dividing PVR progenitors, which are not detected following a sufficiently long chase period due to the dilution of the label over time, but also because of migration away from the region, or cell death [5, 6, 38–40]. Based on a cell cycle time of 12.7
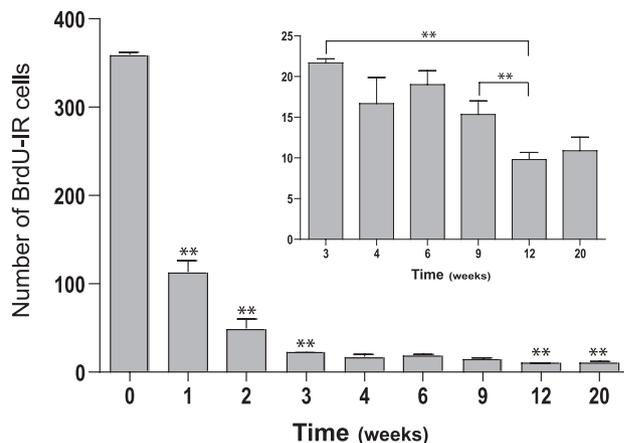
Figure 3. Quantitative analysis of the decline in BrdU-IR cells in the rostral PVR over increasing survival times. The number of BrdU-IR cells present in a 14 μm section (+1.18 mm from Bregma) of the PVR of the rostral lateral ventricle was determined for a 20 week chase period. A decline in the number of BrdU-IR cells was observed over each of the first 3 weeks post-injection ($p < .01$, $n = 3$ each time point, Student's t-test), leaving only 6.05% of the original population (358.3 $\pm$ 4.8 vs. 21.7 $\pm$ 0.5, mean $\pm$ SEM, $n = 3$). A second significant decline in the number of BrdU-IR cells was observed at 12 weeks as compared to the number of BrdU-IR cells detected at 3 weeks (upper bar, $p = .009$, $n = 3$, Student's t-test) and 9 weeks (lower bar, $p = .04$, $n = 3$, Student's t-test), after which no change was detected. Note: Y-axis range reduced in inset to highlight 3–20 week values.

hours (4.2 hour S-phase) for progenitors and approximately 15 days for NSCs [2, 39–42], a brief labeling period (i.e., injections every 2–3 hours for a total of 12 hours) is sufficient to label all of the proliferating progenitors and a fraction of NSCs, with the quantification of labeled NSCs possible within 30 days. By employing this regime - BrdU injections every 3 hours for 12 hours then sacrificing mice 30 days after the last injection, van der Kooy and colleagues [26] recently reported the ability to detect and enumerate NSCs. We chose a slightly modified injection protocol, pulsing mice with BrdU every 2 hours for 48 hours, which extended the window of detection from 12–48 hours so as to label a greater number of slowly dividing cells. This protocol has previously been demonstrated to provide a more comprehensive picture of the mitotic activity of cells in the hippocampus (with no detectable cytotoxicity) as compared to standard single pulse methods [7]. To ascertain whether a 30 day chase remained sufficient to identify LRCs, we counted the number of BrdU-IR cells in a representative region of the rostral lateral ventricles over a 20 week chase period. At each time-point the mean number of BrdU-IR cells detected in the PVR of equivalent tissue sections ($n = 3$ mice for each time point) was calculated and plotted as a function of time. As illustrated in Figure 3, we observed a rapid initial decline in BrdU-IR cells during the first 3 weeks post-injection, presumably reflecting the dilution of the label in constitutively proliferating progenitor cells. The number of BrdU-IR cells then remained unchanged until 12 weeks post-injection, when a second significant decline was observed ($p = .009$, Inset Fig. 3). As no further decline was observed at the final time point assayed (i.e., 20 weeks), we considered the 12 week chase period a reasonable starting point from which to determine the number of LRCs.

Accordingly, a second cohort of mice received BrdU injections over 48 hours (as above) and was sacrificed at chase periods of 3, 5, or 7 months following the last injection. Unlike preliminary experiments where BrdU-IR cells were enumerated from a single representative coordinate (Fig. 3), two major changes in methodology were adopted here. First, rather than

examining a single coordinate, serial cryostat sections were harvested from three mice at each time point and processed so as to overlap with the 23 individual 400 μm segments examined in the in vitro experiments described above. Second, rather than simply enumerating BrdU-IR cells, which would include differentiated cell types, we determined the number of LRCs by subtracting the mean number of BrdU-IR cells expressing differentiated cell markers for neurons (BrdU/NeuN), astrocytes (BrdU/S-100), oligodendrocytes (BrdU/MBP), as well as non-neural cell types including endothelial cells (BrdU/CD31) and blood cell types (BrdU/CD45) from the mean number of BrdU-IR cells detected in the PVR. Glial fibrillary acidic protein (GFAP) was not employed as a marker for differentiated cells here because of the potential exclusion of neural stem cells [41], and more practically because of the filamentous nature of the labeling, which makes the identification of double-label coincidences (i.e., BrdU/GFAP) exceedingly difficult. Somewhat surprisingly, the fraction of BrdU-labeled cells immunoreactive for differentiated cell types did not exceed 3% at any time point or coordinate, nor did we detect any newly generated oligodendrocytes within the PVR (Fig. 4). We also failed to detect an appreciable number (i.e., < 0.1%) of BrdU-IR endothelial cells (CD31) or hematopoietic cell types (using the pan-blood cell marker CD45) within the PVR.

Consistent with our preliminary observation of BrdU-IR cells, we did not detect a significant decline in LRC number between the 3 and 5 month chase periods at the representative coordinate previously examined for BrdU-IR cell decline (+1.18 Bregma, Fig. 3A), nor within the 400 μm region containing the representative coordinate (i.e., section 10, Fig. 4) ($p = .02$, $n = 3$). However, a significant decline in the absolute number of LRCs detected throughout the neuraxis at 3 versus 5 month (6,953 ± 190 vs. 5,292 ± 102, $p = .01$) and 5 versus 7 month (5,292 ± 102, $p = .01$ vs. 1,186 ± 188, $p < .001$, $n = 3$, Student's t-test) chase periods was apparent (Fig. 4). Of interest, a comparison of LRC frequency in individual sections across all three chase periods (as opposed to the entire neuraxis) revealed that the number of LRCs in only four sections (10–11 and 19–20) declined significantly across all three chase periods.

## Proliferative Potential of LRCs

Whereas technical difficulties relating to dilution of the BrdU label over time prevented us from using the N-CFCA to test directly what proportion of LRCs were stem cell derived (i.e., >2 mm), it was possible to determine what proportion of LRCs could generate neurospheres [43]. Accordingly, brains were harvested and sectioned from BrdU-injected mice 5 months after the last injection. Cells were harvested from the PVR in a single vibratome section (section 11), where the frequency of sphere-forming (676 ± 129), colony-forming (891 ± 87), and label-retaining cells (931 ± 115) were previously demonstrated not to differ significantly ($p > .05$, $n = 3$, Student's t-test), and cultured in the neurosphere assay. After an abbreviated period in culture (4 vs. 7-10 DIV so as to limit the dilution of the BrdU label) the cultures were fixed and processed so as to detect BrdU-IR cells within individual neurospheres. As illustrated in Figure 5, 37 primary neurospheres of the 811 generated (4.52 ± 0.44%, $n = 3$) contained at least one BrdU-IR cell, suggesting these were LRC-derived. Because of this unexpectedly low number we re-examined cryostat sections harvested from the same cohort of 5-month-chase mice (and from the same region), performing double-label immunocytochemistry for BrdU and Ki-67, a protein present during all active phases of the cell cycle (G_1, S, G_2, M) but absent in resting (G_0) cells [44], to determine what percentage of LRCs were mitotically active. We also
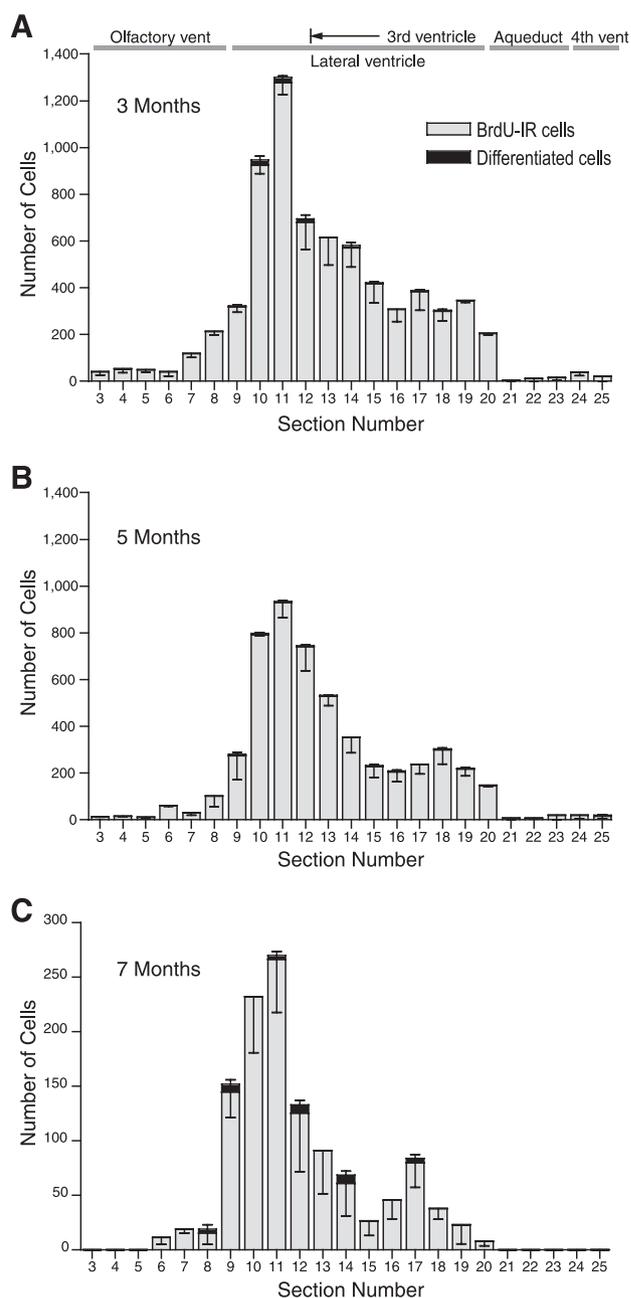
Figure 4. Distribution of label-retaining cells along the ventricular neuraxis. Brains were harvested and serially sectioned from BrdU-injected mice at 3 months **(A)**, 5 months **(B)**, and 7 months **(C)** following the last injection ($n = 3$ mice for each time point). The number of LRCs was determined for individual 400 μm regions by subtracting the mean number of BrdU-IR differentiated cells (i.e., BrdU/NeuN, BrdU/S-100, BrdU/MBP; Differentiated cells) from the mean number of BrdU-IR cells (BrdU-IR cells) detected in five individual tissue sections, spanning a 420 μm segment of the brain. Similar to the findings for SFCs (Fig. 1A), the majority of LRCs were located in sections 9–14 (63%, 68%, and 78% for 3, 5, and 7 month chase periods, respectively). A significant decline was observed in the overall number of LRCs between 3 (6,953 ± 351, mean ± SEM $n = 3$) and 5 month (5,292 ± 102, $n = 3$) ($p = .01$, Student's t-test), and 5 versus 7 month (1,186 ± 188, $n = 3$) chase periods ($p < .001$, Student's t-test). Note: positive error bars reflect mean ± SEM for differentiated cells, whereas negative error bars reflect mean ± SEM for BrdU-IR cells.

double-labeled for BrdU and Mcm-2, a marker previously employed to detect slow-cycling putative NSCs in situ [38] as it
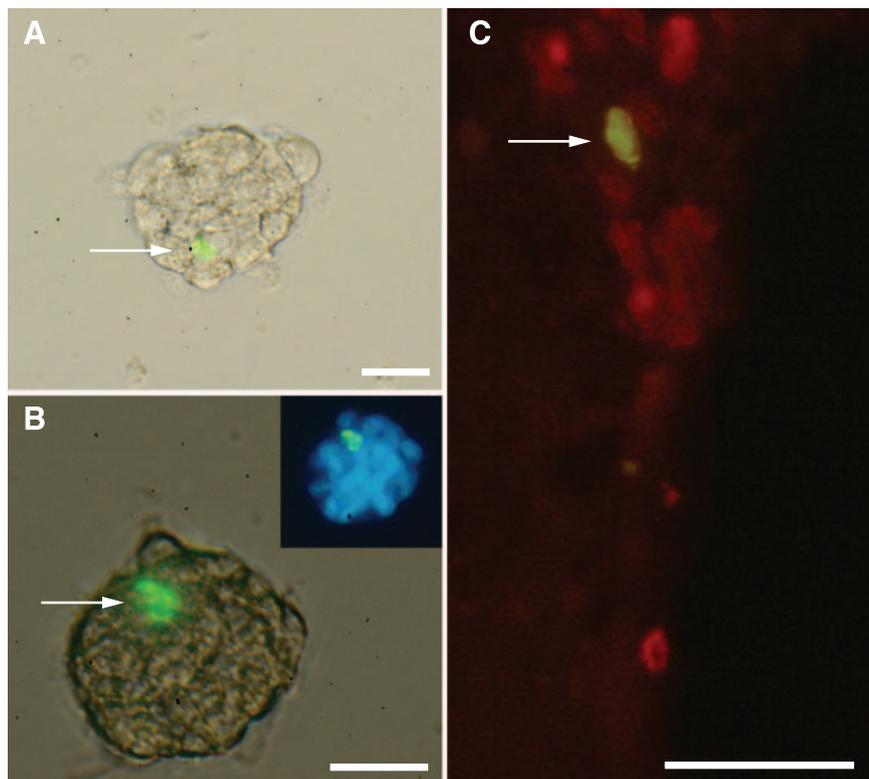
Figure 5. A minority of LRCs can divide to generate primary neurospheres or retain the ability to divide. **(A, B)** Photomicrographs of representative primary neurospheres generated from BrdU-recipient mice 5 months post-injection containing BrdU-IR cells (arrows). **(Inset)** Neurosphere shown in **(B)** counterstained with DAPI (blue). **(C)** Cryostat tissue section (14 μm) of the PVR along the lateral wall of the left lateral ventricle also taken from BrdU-recipient mice 5 months post-injection. Although numerous BrdU-IR cells (red) are present in the PVR, only one is also immunoreactive for Mcm2 (green) and thus competent to divide at the time of harvest. Scale bars = 20 μm.

labels a pre-replication complex protein found in cells competent for the initiation of replication but not actively dividing (i.e., cells in G_0 and G_1) [45, 46]. Consistent with approximately 5% of LRCs possessing the capacity to generate neurospheres, 5.49 $\pm$ 1.0% ($n = 3$) of BrdU-IR cells detected in the PVR 5 months following the last injection were double-labeled with Ki-67, while 7.69 $\pm$ 2.1% ($n = 3$) of BrdU-IR cells were double-labeled with Mcm-2. Taken together, these data suggest that only a small minority of the LRCs (approximately 5–10%) present in this region of the ventricular wall are actively cycling, or are competent to divide 5 months after their labeling with the mitotic cell marker BrdU.

DISCUSSION

Consistent with previous work, we detected SFCs in the PVR of the olfactory bulb [36], lateral, third and fourth ventricles [2, 34, 47]. Also consistent with previous work [34], but described in much greater detail (Fig. 1, Fig. 6), we found that the absolute number and frequency of SFCs varies considerably along the neuraxis. These differences are most striking in the rostral portion of the lateral ventricle, the region originally harvested by Reynolds and Weiss [1] and most frequently used in subsequent studies employing the neurosphere assay. This serves to explain the wide range of primary neurosphere numbers generated by different groups employing the same basic tissue harvest techniques.

A brief survey of published work revealed that the number of primary neurospheres generated in a typical dissection (i.e., encompassing sections 9–14) ranges between 150 and 936 [36, 41, 42, 48], whereas we generated approximately 2,700 primary neurospheres from the same region. Several factors may account for this. First, our primary dissection encompasses essentially the entire PVR, resulting in a greater number of SFCs harvested. Second, our precise dissection of the PVR minimizes unwanted

parenchymal tissue, which inhibits primary sphere formation (data not shown). It also results in smaller pieces of tissue, enabling abbreviated enzymatic digestion and trituration, minimizing cell loss. Our defining criteria of a neurosphere (i.e., those clusters of cells $\geq$50 μm) varies from that of previous reports, which enumerated those spheres >50 μm [16], $\geq$100 μm [25], or $\geq$120 μm [14]. These discrepancies highlight the need for greater diligence and improved techniques when generating adult neurospheres.

As illustrated in Figure 6, the distribution and frequency of colony formation essentially mirrored that of neurosphere generation along the entire neuraxis. Given no significant difference was found between the total numbers of colonies/spheres generated (4,275 $\pm$ 124 vs. 3,730 $\pm$ 276, $p = .08$, $n = 3$), these results suggest that each assay is detecting overlapping proliferative populations. Based on prior work demonstrating that only those colonies >2 mm are NSC-derived [27] (i.e., exhibit cardinal stem cell attributes in vitro), we now conclude that NSC-derived colonies comprise approximately 1.2% of the total colonies detected (50 $\pm$ 10 of 4,275 $\pm$ 124 detected, Fig. 2B). To our knowledge only one prior estimate of the number of endogenous NSCs in the PVR has been reported. Morshead and colleagues [39] performed an arduous in vivo lineage analysis of individual clones that had been labeled with a replication-deficient retrovirus (containing a β-galactosidase reporter gene). By determining the incidence of the largest clones (i.e., those containing 28 cells or more, which were considered NSC-derived) within the PVR following the ablation and repopulation of the subependyma (during which NSCs are activated [2]), they calculated the number of NSCs that were present in the forebrain to be 1,238, constituting 0.4% of the entire subependymal population. This figure is most likely an overestimate, given their calculations are based on the assumption that 50%, which represents the maximum value possible in light of the data presented of normally quiescent endogenous
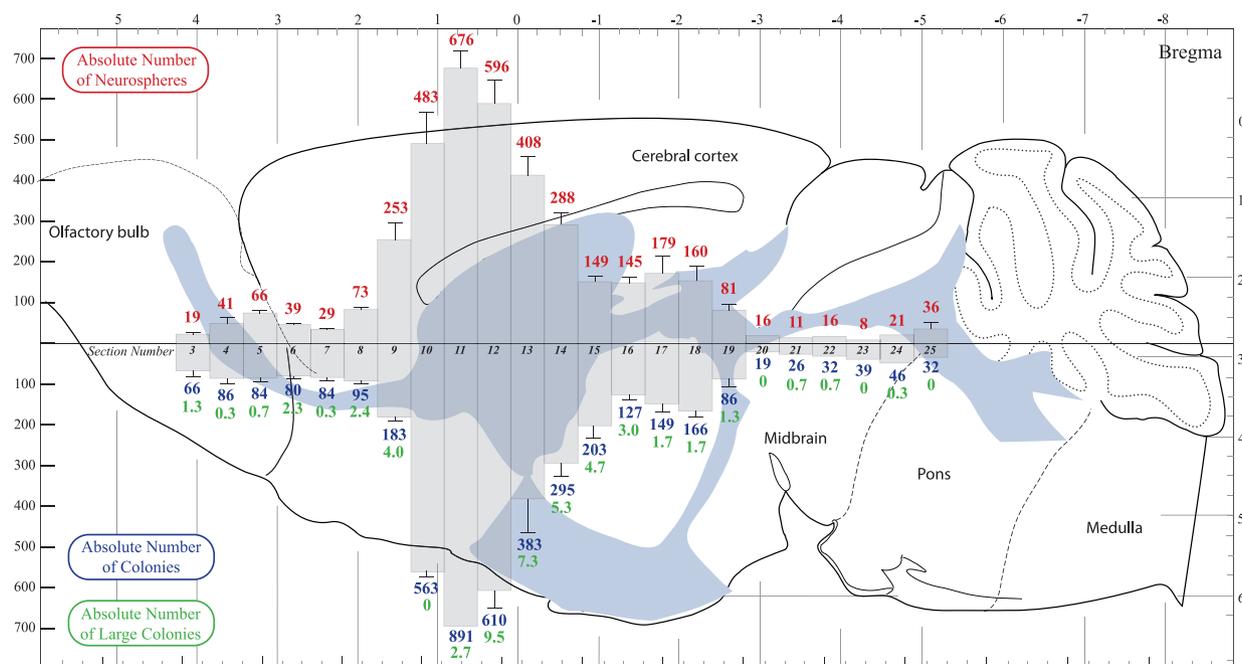
Figure 6. Map of neural stem and progenitor cell prevalence along the ventricular neuraxis of the adult mouse brain. The number of primary SFCs (upper histogram) and CFCs (regardless of size, lower histogram) detected in 23 individual 400 μm vibratome sections (*Section Number 3–25*) along the ventricular system as observed in a virtual saggital section with the ventricular neuraxis in a single plane. The absolute number of SFCs (red) detected in individual sections essentially mirrors the number of CFCs (blue) detected in comparable sections. The same cannot be said for large colonies (green), which are absent in some regions.

NSCs are activated 2 days following the depletion of constitutively proliferating cells [2].

Rather than being located throughout the neuraxis, we now report that four regions along the rostral-caudal axis of the PVR (sections 10, 20, 23 and 25, Fig. 2B) are devoid of NSCs (i.e., large colonies). This finding was especially unexpected (yet consistent with the absence of a 1:1 relationship between SFCs and NSCs [17]) in section 10, given the large number of primary neurospheres 483 ± 84 (Fig. 1A) that were generated from the region. The inability of neurosphere cultures generated from this section to be serially passaged over an extended period of time suggests this is not a peculiarity of the N-CFCA, but rather, may reflect an absence of NSCs [29, 49]. The significance of these "gaps" along the neuraxis is unclear. It is tempting to believe that their location is not random, as sections 10, 20 and 25 correspond to the coordinates of the cephalic flexures in the developing brain, becoming the rostral boundary of the ventricular neuraxis in the forebrain (+1.34 Bregma), midbrain (−2.92 Bregma) and hindbrain (−5.34 Bregma) in the adult. If these "gaps" represent boundaries established during development, it suggests that same factors that control regional specialization influence the generation of distinct populations of NSCs in the adult. Further study into the significance of this finding is warranted, but this lies outside the scope of the present study.

Our analysis of the ability of the LRC technique to discriminate between stem and progenitor cells did not provide sufficient evidence to warrant a definitive conclusion to be made. In other organs in the body, several disparate lines of evidence have been gathered to support the claim that LRC technology can be used to selectively identify or purify tissue stem cells. For instance, in the hair follicle, LRCs represent a rare population of cells that is activated in situ following injury, generating differentiated progeny and ultimately regenerating the tissue [20, 50]. In addition, when transferred to culture, LRCs proliferate to form clusters or "spheres", which contain multiple differentiated cell types [51]. Taken together, these published observations

argue that stem cells are identified as part of the LRC population, but they do not support the claim that this technique can be used to selectively identify stem cells, specifically enrich for stem cells, or that all LRCs are stem cells.

The same is true of the LRCs identified here. We demonstrate that they represent a rare population of cells (Fig. 3) residing in the NSC-enriched PVR, approximately 5% of which are slow cycling (BrdU$^+$/Ki-67$^+$) or relatively quiescent (BrdU$^+$/Mcm-2$^+$), and proliferate upon transfer to culture (Fig. 5). Unfortunately, given that a) the phenotype of a NSC is currently unknown, b) NSC-specific markers are unavailable, c) the sorting techniques previously reported to enrich for NSCs used the neurosphere assay as a read-out for stem cell activity, and d) it remains unclear whether the N-CFCA (or other tissue culture techniques) accurately detects the complement of endogenous NSCs found in the adult mammalian brain, little more can be concluded.

Whereas only a portion of the LRC population remains competent to divide, this evidence cannot unequivocally support or refute the hypothesis that the LRC technique can be used to selectively identify or specifically enrich for NSCs. Given that exposure to increasing concentrations of BrdU is known to cause a gradient of cytotoxic effects [7], it is also possible that the incorporation BrdU may account for the inability of the LRCs to proliferate. In this regard we favor our approach in comparison to the double nucleoside labeling strategy, which has also been applied to detect relatively quiescent NSCs [25, 38]. In this case the nucleoside analogs 5-iodo-2-deoxyuridine (IdU) and 5-chloro-2-deoxyuridine (CldU), which can be detected independently, are used in a double labeling manner to determine whether putative LRCs will re-enter the cell cycle. Although both methods would be equally effective in detecting relatively quiescent cells, we believe that the increased risk of cytotoxic damage associated with the incorporation of a second analog in the mitotically active LRCs would outweigh the extended window of detection this latter approach would afford.

Unfortunately, neither technique enables the direct demonstration that the labeled cells are bona fide stem cells rather than progenitor cells. As such, we contend that caution should be taken with the interpretation of data pertaining to LRCs regardless of the specific technique employed.

Although a number of markers including but not limited to Nestin, Musashi, GFAP, and NG2 have been reported to co-localize with NSCs [41, 52–54], none of these have been demonstrated to be expressed exclusively by NSCs, thereby precluding their use to selectively distinguish stem from progenitor cells. Stem cell sorting strategies based on unique cell surface antigen expression [11–14], Hoechst dye exclusion [15, 55] or aldehyde dehydrogenase activity [56] have to date employed the neurosphere assay as a read-out of stem cell activity, leaving the purity of the final population in doubt. With the exception of generating long-term neurosphere cultures from each individual primary neurosphere generated (in this case approximately 3,730, Fig. 1), then assaying for cardinal stem cell attributes, we are not aware of any strategy that will enable a more detailed analysis (or provide further support) of the frequency and distribution of NSCs reported here.

CONCLUSION

Our analysis of the in vivo location of stem and progenitor cells along the ventricular neuraxis revealed that the distribution of progenitors was remarkably consistent as detected by the neurosphere assay and N-CFCA, but the number and location of NSCs varied to a large degree depending upon the assay employed. Besides providing a benchmark, our analysis more importantly highlights the need for greater precision and caution when employing these methodologies to investigate NSCs and progenitor cells in the adult mouse brain. As always, careful consideration should be given that the techniques and anatomical location chosen are appropriate for the question being investigated.

ACKNOWLEDGMENTS

DISCLOSURE OF POTENTIAL CONFLICTS OF INTEREST

The authors indicate no potential conflicts of interest.

REFERENCES

1 Reynolds BA, Weiss S. Generation of neurons and astrocytes from isolated cells of the adult mammalian central nervous system. Science 1992;255:1707–1710.
2 Morshead CM, Reynolds BA, Craig CG et al. Neural stem cells in the adult mammalian forebrain: a relatively quiescent subpopulation of subependymal cells. Neuron 1994;13:1071–1082.
3 Gage FH. Mammalian neural stem cells. Science 2000;287:1433–1438.
4 Altman J. Are neurons formed in the brains of adult mammals? Science 1962;135:1127–1128.
5 Luskin M. Restricted proliferation and migration of postnatally generated neurons derived from the forebrain subventricular zone. Neuron 1993; 11:173–189.
6 Lois C, Alvarez-Buylla A. Long-distance neuronal migration in the adult mammalian brain. Science 1994;264:1145–1148.
7 Rietze R, Poulin P, Weiss S. Mitotically active cells that generate neurons and astrocytes are present in multiple regions of the adult mouse hippocampus. J Comp Neurol 2000;424:397–408.
8 Ming GL, Song H. Adult neurogenesis in the mammalian central nervous system. Annu Rev Neurosci 2005;28:223–250.
9 Emsley JG, Mitchell BD, Kempermann G et al. Adult neurogenesis and repair of the adult CNS with neural progenitors, precursors, and stem cells. Prog Neurobiol 2005;75:321–341.
10 Thored P, Arvidsson A, Cacci E et al. Persistent production of neurons from adult brain stem cells during recovery after stroke. STEM CELLS 2006;24:739–747.
11 Capela A, Temple S. LeX/ssea-1 is expressed by adult mouse CNS stem cells, identifying them as nonependymal. Neuron 2002;35:865–875.
12 Rietze RL, Valcanis H, Brooker GF et al. Purification of a pluripotent neural stem cell from the adult mouse brain. Nature 2001;412:736–739.
13 Uchida N, Buck DW, He D et al. Direct isolation of human central nervous system stem cells. Proc Natl Acad Sci USA 2000;97:14720–14725.
14 Young KM, Merson TD, Sotthibundhu A et al. p75 neurotrophin receptor expression defines a population of BDNF-responsive neurogenic precursor cells. J Neurosci 2007;27:5146–5155.
15 Kim M, Morshead CM. Distinct populations of forebrain neural stem and progenitor cells can be isolated using side-population analysis. J Neurosci 2003;23:10703–10709.
16 Murayama A, Matsuzaki Y, Kawaguchi A et al. Flow cytometric analysis of neural stem cells in the developing and adult mouse brain. J Neurosci Res 2002;69:837–847.
17 Reynolds BA, Rietze RL. Neural stem cells and neurospheres–re-evaluating the relationship. Nat Methods 2005;2:333–336.
18 Kenney NJ, Smith GH, Lawrence E et al. Identification of stem cell units in the terminal end bud and duct of the mouse mammary gland. J Biomed Biotechnol 2001;1:133–143.
19 Morris RJ, Potten CS. Slowly cycling (label-retaining) epidermal cells behave like clonogenic stem cells in vitro. Cell proliferation 1994;27: 279–289.
20 Morris RJ, Potten CS. Highly persistent label-retaining cells in the hair follicles of mice and their fate following induction of anagen. J Invest Derm 1999;112:470–475.
21 Oliver JA, Maarouf O, Cheema FH et al. The renal papilla is a niche for adult kidney stem cells. J Clin Invest 2004;114:795–804.
22 Potten CS, Loeffler M. Stem cells: attributes, cycles, spirals, pitfalls and uncertainties. Lessons for and from the crypt. Development 1990;110: 1001–1020.
23 Quesenberry P, Levitt L. Hematopoietic stem cells. N Engl J Med 1979;301:755–761.
24 Tumbar T, Guasch G, Greco V et al. Defining the epithelial stem cell niche in skin. Science 2004;303:359–363.
25 Bauer S, Patterson PH. Leukemia inhibitory factor promotes neural stem cell self-renewal in the adult brain. J Neurosci 2006;26:12089–12099.
26 Kippin TE, Martens DJ, van der Kooy D. p21 loss compromises the relative quiescence of forebrain stem cell proliferation leading to exhaustion of their proliferation capacity. Genes Dev 2005;19:756–767.
27 Louis SA, Rietze RL, Deleyrolle L et al. Enumeration of neural stem and progenitor cells in the neural colony forming cell assay. STEM CELLS 2008; In Press.
28 Young KM, Fogarty M, Kessaris N et al. Subventricular zone stem cells are heterogeneous with respect to their embryonic origins and neurogenic fates in the adult olfactory bulb. J Neurosci 2007;27:8286–8296.
29 Bull ND, Bartlett PF. The adult mouse hippocampal progenitor is neurogenic but not a stem cell. J Neurosci 2005;25:10815–10821.
30 Paxinos G, Franklin KBJ. The Mouse Brain in Stereotaxic Coordinates. Academic Press; 2001.
31 Rietze RL, Reynolds BA. Neural stem cell isolation and characterization. Methods Enzymol 2006;419:3–23.
32 Altman J. Autoradiographic investigation of cell proliferation in the brains of rats and cats. Anat Rec 1963;145:573–591.
33 Smart I. The subependymal layer of the mouse brain and its cell production as shown by radioautography after thymidine-H³ injection. J Comp Neurol 1961;116:325–347.
34 Weiss S, Dunne C, Hewson J et al. Multipotent CNS stem cells are present in the adult mammalian spinal cord and ventricular neuroaxis. J Neurosci 1996;16:7599–7609.
35 Morshead CM, van der Kooy D. Disguising adult neural stem cells. Curr Opin Neurobiol 2001;14:125–131.
36 Gritti A, Bonfanti L, Doetsch F et al. Multipotent neural stem cells reside into the rostral extension and olfactory bulb of adult rodents. J Neurosci 2002;22:437–445.

37 Sohur US, Emsley JG, Mitchell BD et al. Adult neurogenesis and cellular brain repair with neural progenitors, precursors and stem cells. Philos Trans R Soc Lond B Biol Sci 2006;361:1477–1497.

38 Maslov AY, Barone TA, Plunkett RJ et al. Neural stem cell detection, characterization, and age-related changes in the subventricular zone of mice. J Neurosci 2004;24:1726–1733.

39 Morshead CM, Craig CG, van der Kooy D. In vivo clonal analyses reveal the properties of endogenous neural stem cell proliferation in the adult mammalian forebrain. Development 1998;125:2251–2261.

40 Morshead CM, van der Kooy D. Postmitotic death is the fate of constitutively proliferating cells in the subependymal layer of the adult mouse brain. J Neurosci 1992;12:249–256.

41 Doetsch F, Caille I, Lim DA et al. Subventricular zone astrocytes are neural stem cells in the adult mammalian brain. Cell 1999;97:703–716.

42 Tropepe V, Craig CG, Morshead CM et al. Transforming growth factor-alpha null and senescent mice show decreased neural progenitor cell proliferation in the forebrain subependyma. J Neurosci 1997; 17:7850–7859.

43 Ferron SR, Andreu-Agullo C, Mira H et al. A combined ex/in vivo assay to detect effects of exogenously added factors in neural stem cells. Nature Protocols 2007;2:849–859.

44 Scholzen T, Gerdes J. The Ki-67 protein: from the known and the unknown. J Cell Physiol 2000;182:311–322.

45 Stillman B. Cell cycle control of DNA replication. Science 1996;274: 1659–1664.

46 Ritzi M, Knippers R. Initiation of genome replication: assembly and disassembly of replication-competent chromatin. Gene 2000;245:13–20.

47 Chiasson BJ, Tropepe V, Morshead CM et al. Adult mammalian forebrain ependymal and subependymal cells demonstrate proliferative potential, but only subependymal cells have neural stem cell characteristics. J Neurosci 1999;19:4462–4471.

48 Enwere E, Shingo T, Gregg C et al. Aging results in reduced epidermal growth factor receptor signaling, diminished olfactory neurogenesis, and deficits in fine olfactory discrimination. J Neurosci 2004;24:8354–8365.

49 Seaberg RM, van der Kooy D. Adult rodent neurogenic regions: the ventricular subependyma contains neural stem cells, but the dentate gyrus contains restricted progenitors. J Neurosci 2002;22:1784–1793.

50 Lavker RM, Sun TT. Epidermal stem cells: properties, markers, and location. Proc Natl Acad Sci USA 2000;97:13473–13475.

51 Claudinot S, Nicolas M, Oshima H et al. Long-term renewal of hair follicles from clonogenic multipotent stem cells. Proc Natl Acad Sci USA 2005;102:14677–14682.

52 Kaneko Y, Sakakibara S, Imai T et al. Musashi1: an evolutionally conserved marker for CNS progenitor cells including neural stem cells. Dev Neurosci 2000;22:139–153.

53 Aguirre A, Rizvi TA, Ratner N et al. Overexpression of the epidermal growth factor receptor confers migratory properties to nonmigratory postnatal neural progenitors. J Neurosci 2005;25:11092–11106.

54 Yokoyama A, Sakamoto A, Kameda K et al. NG2 proteoglycan-expressing microglia as multipotent neural progenitors in normal and pathologic brains. Glia 2006;53:754–768.

55 Mouthon MA, Fouchet P, Mathieu C et al. Neural stem cells from mouse forebrain are contained in a population distinct from the 'side population'. J Neurochem 2006;99:807–817.

56 Corti S, Locatelli F, Papadimitriou D et al. Identification of a primitive brain-derived neural stem cell population based on aldehyde dehydrogenase activity. STEM CELLS 2006;24:975–985.

This information is current as of April 29, 2008

Updated Information & Services	including high-resolution figures, can be found at: http://www.StemCells.com/cgi/content/full/26/4/979

AlphaMed Press